END

FILMED

DTIC

MICROCOPY RESOLUTION TEST CHART
NATIONAL BUREAU OF STANDARDS-1963-A

AD-A162 194

REPORT DOCUMENTATION PAGE		READ INSTRUCTIONS BEFORE COMPLETING FORM
1. REPORT NUMBER AFOSR-TR- 85 - 1017	2. GOVT ACCESSION NO. AD-A162 194	3. RECIPIENT'S CATALOG NUMBER
4. TITLE *(and Subtitle)* Nonlinear Analysis and Optimal Design of Dynamic Mechanical Systems for Spacecraft Application		5. TYPE OF REPORT & PERIOD COVERED Annual Technical Report Feb. 1, 1984 - Jan. 31, 1985
		6. PERFORMING ORG. REPORT NUMBER
7. AUTHOR(s) K. D. Willmert and M. Sathyamoorthy		8. CONTRACT OR GRANT NUMBER(s) AFOSR-84-0076
9. PERFORMING ORGANIZATION NAME AND ADDRESS Clarkson University Potsdam, New York 13676		10. PROGRAM ELEMENT, PROJECT, TASK AREA & WORK UNIT NUMBERS 61102F 2302/B1
11. CONTROLLING OFFICE NAME AND ADDRESS Air Force Office of Scientific Research /NA Washington, D.C.		12. REPORT DATE February 1985
		13. NUMBER OF PAGES 54
14. MONITORING AGENCY NAME & ADDRESS *(if different from Controlling Office)*		15. SECURITY CLASS. *(of this report)* Unclassified
		15a. DECLASSIFICATION/DOWNGRADING SCHEDULE

16. DISTRIBUTION STATEMENT *(of this Report)*

Approved for public release; distribution unlimited.

17. DISTRIBUTION STATEMENT *(of the abstract entered in Block 20, if different from Report)*

DTIC
ELECTE
DEC 0 9 1985
E

18. SUPPLEMENTARY NOTES

19. KEY WORDS *(Continue on reverse side if necessary and identify by block number)*

Mechanisms, vibrational analysis, optimization, geometric nonlinearity, material nonlinearity,

20. ABSTRACT *(Continue on reverse side if necessary and identify by block number)*

A nonlinear finite element procedure has been developed for the dynamic vibrational analysis of planar mechanisms. The analysis takes into account the effects of geometric and material nonlinearities, vibrational effects and coupling of deformations. Numerical results have been reported for certain mechanism examples. The effects of the nonlinearities have been found to be significant on the dynamic behavior. Due to the complex nature of this nonlinear analysis procedure, an efficient optimal design approach

DD FORM 1473 EDITION OF 1 NOV 65 IS OBSOLETE
1 JAN 73
S/N 0102-LF-014-6601

Approved for public release;
distribution unlimited.

using an optimality criterion technique has also been developed. The new optimization technique, called the Gauss Nonlinearly Constrained Technique, has been developed in such a way that it is applicable to design problems with nonlinear objective functions and constraints. The applicability of this method has been demonstrated with example problems consisting of objective functions of various complexities. Complete details of the nonlinear finite element procedure as well as the optimization technique are available in two papers (to be published) which are included here in the Appendix.

Accession For	
NTIS GRA&I	☒
DTIC TAB	☐
Unannounced	☐
Justification	
By	
Distribution/	
Availability Codes	
Dist	Avail and/or Special
A-1	

Annual Technical Report

February 1, 1984 through January 31, 1985

NONLINEAR ANALYSIS AND OPTIMAL DESIGN OF DYNAMIC MECHANICAL

SYSTEMS FOR SPACECRAFT APPLICATION

Principal Investigators:

K.D. Willmert

and

M. Sathyamoorthy

Department of Mechanical and

Industrial Engineering

Clarkson University

Potsdam, New York 13676

February 1985

Summary

A nonlinear finite element procedure has been developed for the dynamic vibrational analysis of planar mechanisms. The analysis takes into account the effects of geometric and material nonlinearities, vibrational effects and coupling of deformations. Numerical results have been reported for certain mechanism examples. The effects of the nonlinearities have been found to be significant on the dynamic behavior. Due to the complex nature of this nonlinear analysis procedure, an efficient optimal design approach using an optimality criterion technique has also been developed. The new optimization technique, called the Gauss Nonlinearly Constrained Technique, has been developed in such a way that it is applicable to design problems with nonlinear objective functions and constraints. The applicability of this method has been demonstrated with example problems consisting of objective functions of various complexities. Complete details of the nonlinear finite element procedure as well as the optimization technique are available in two papers (to be published) which are included here in the Appendix.

Research Objectives

The objectives of this research are to develop a nonlinear finite element dynamic analysis procedure for both planar and spatial mechanisms of the type found in space structures. Geometric, and material nonlinearities as well as combinations of these are to be included in the analysis. Furthermore, an efficient optimal design method is to be developed to handle objective functions composed of a combination of rigid body and deformation displacements involving

1

geometric design variables as well as cross-sectional sizes. Thus, during the
reporting period it was proposed to

      a) develop a nonlinear finite element procedure for dynamic planar
         mechanisms;

      b) develop an efficient optimization method involving a small number of
         analyses for mechanism design problems.

Significant Accomplishments

Substantial progress has been made in both of these two research areas
during the reporting period. Complete details of the work are included in the
Appendix; only a summary is presented here.

In the nonlinear finite element analysis area, planar mechanism problems
have been formulated to include the effects of material and geometric
nonlinearities due to large deformations, and vibrational effects for members
with nonuniform cross sections. Effects of transverse shear and rotatory
inertia have also been included. Numerical results for deformations and
stresses have been reported for certain planar mechanisms. The results clearly
indicate the effects of geometric and material nonlinearities on the dynamic
behavior of planar mechanisms and the need to include these effects in the
analysis.

In the optimal design area, a new optimization technique, called the Gauss
Nonlinearly Constrained Method (GNLC), which is applicable to design problems
with nonlinear objective functions and constraints has been developed. The GNLC
technique is an extension of a previously developed method called the Gauss
Constrained Technique which is capable of handling only linear constraints.
Both of these techniques, based on Gauss' unconstrained method, were developed

so that the Kuhn-Tucker conditions were automatically satisfied when the procedure terminated. As an example, a four-bar mechanism was designed such that the coupler point (XX,YY) of the mechanism closely generated a curve defined by discrete points. The objective function to be minimized in this case was the sum of the distances (squared) between the desired curve and the actual curve generated by the mechanism. This objective function is a highly nonlinear function of the design variables. For the particular example considered, the GNLC technique was found to require significantly fewer objective function and constraint evaluations than currently available methods.

Publications

a) Technical Reports:

1. D.R. Boston, K.D. Willmert and M. Sathyamoorthy, "The Gauss Nonlinearly Constrained Method Applied to Mechanism Design," Department of Mechanical and Industrial Engineering, Clarkson University, Potsdam, NY, Report No. MIE-104, June 1984.

2. D.W. Tennant, K.D. Willmert and M. Sathyamoorthy, "Vibration of Mechanisms with Material and Geometric Nonlinearities Using Variable Length Finite Elements," Department of Mechanical and Industrial Engineering, Clarkson University, Potsdam, NY, Report No. MIE-106, October 1984.

b) Technical Journals, Meetings, Conferences

1. K.D. Willmert and M. Sathyamoorthy, "Optimal Design of Flexible Mechanisms," Presented at the Second Forum on Space Structures, McLean Virginia, June 11-13, 1984.

2. D.R. Boston, K.D. Willmert and M. Sathyamoorthy, "Gauss' Nonlinearly Constrained Optimization Method," Proceedings of the ASCE Engineering Mechanics Specialty Conference, University of Wyoming, Laramie, August 1984, pp. 82-85.

3. K.D. Willmert and M. Sathyamoorthy, "Optimal Design of Dynamic Mechanical Systems Undergoing Large Deformations," Paper presented at the Conference on Super Computers in Mechanical Systems Research, Lawrence Livermore Laboratory, Livermore, California, September 1984.

4. D.R. Boston, K.D. Willmert and M. Sathyamoorthy, "The Development and Application of Gauss' Nonlinearly Constrained Optimization Method,"

Submitted for Publication in Journal of Structural Mechanics, December 1984.

5. D.W. Tennant, K.D. Willmert and M. Sathyamoorthy, "Finite Element Nonlinear Analysis of Planar Mechanisms," Submitted for Publication in Journal of Mechanism and Machine Theory, February 1985.

6. Edward Kear III, M. Sathyamoorthy and K.D. Willmert, "Vibration Analysis of Mechanisms with Geometric and Material Nonlinearities," Accepted for Presentation at the ASME Symposium on Material Nonlinearity in Vibration Problems, ASME Winter Annual Meeting, Miami Beach, Florida, November 1985 (Also Submitted for Publication in the Symposium Volume).

7. Edward Kear III, M. Sathyamoorthy and K.D. Willmert, "Effects of Material Nonlinearity on Vibrations of Beams," to be Submitted to Journal of Sound and Vibration.

Professional Personnel

1. K.D. Willmert, Professor of Mechanical and Industrial Engineering.

2. M. Sathyamoorthy, Associate Professor of Mechanical and Industrial Engineering.

3. D.R. Boston, Completed his Master of Science Degree on May 23, 1984, with thesis entitled, "Development and Application of the Gauss Nonlinearly Constrained Technique to Optimal Four-Bar Mechanism Design."

4. D.W. Tennant, Completed his Master of Science Degree on October 4, 1984, with thesis entitled, "Nonlinear Vibrations of Mechanisms with Material and Geometric Nonlinearities Using Variable Length Finite Elements."

5. T.E. Potter, Currently a Ph.D. student in Mechanical and Industrial Engineering with research topic in optimal design of mechanisms.

6. E.B. Kear III, Currently a Ph.D. student in Mechanical and Industrial Engineering with research topic in nonlinear analysis of mechanisms.

APPENDIX

Paper No. 1 - The Development and Application of Gauss' Nonlinearly Con-
strained Optimization Method by D.R. Boston, K.D. Willmert
and M. Sathyamoorthy

Paper No. 2 - Finite Element Nonlinear Vibration Analysis of Planar Mechanisms
by D.W. Tennant, K.D. Willmert and M. Sathyamoorthy

THE DEVELOPMENT AND APPLICATION OF
GAUSS' NONLINEARLY CONSTRAINED OPTIMIZATION METHOD

D.R. Boston*, K.D. Willmert*
and M. Sathyamoorthy*

Abstract

Presented in this paper is a new optimization technique, called the Gauss Nonlinearly Constrained Technique which is applicable to design problems with nonlinear objective functions and constraints. The technique is an extension of a previously developed method for linear constraints, referred to as the Gauss Constrained Technique. Both of these techniques, based on Gauss' unconstrained method, have been developed so that the Kuhn-Tucker conditions are automatically satisfied when the procedure terminates.

Introduction

The optimal design of many structures and mechanical mechanisms involves one or more complex and time consuming analyses at each iteration of the optimization. This is particularly critical if a large deformation nonlinear analysis is required. In these cases especially, it is important that the optimization method require very few analyses, even at the expense of significantly increasing the amount of calculations by the optimization technique itself. For example in a recent work, DeRubes and Willmert [1] applied the relatively efficient Generalized Reduced Gradient (GRG) Technique of Lasdon et.al [2] to mechanism design for path generation and rigid body guidance. The mechanism links were considered

*Mechanical and Industrial Engineering Department, Clarkson University, Potsdam, N.Y. 13676.

flexible, and thus a quasi-static (linear) finite element analysis was used to obtain deformations and stresses. The GRG required as many as 14,000 mechanism analyses to obtain the optimal design. Computation time approached twenty hours on an IBM 4341 mainframe computer. If a nonlinear analysis had been used, the corresponding times would have been considerably higher.

To reduce the number of analyses, Paradis and Willmert [3] developed a new direct method for efficient design of mechanisms. Gauss' method, which Wilde [4] concluded to be very efficient for unconstrained mechanism design, was modified to handle linear constraints. The resulting technique, referred to as the Gauss Constrained Technique, was highly efficient and required very few objective function evaluations to obtain an optimal design. Their method has been extended, in this paper, to handle nonlinear constraints.

Development of the Method

The optimization problem consists of minimizing:

$$F(\vec{x}) = \vec{\phi}^T \vec{\phi} \tag{1}$$

where $\vec{\phi}$ is a vector of general functions of the variables $\vec{x}$. Many optimal design problems have objective functions of this form. For the derivation of the optimization technique, the ϕ's are approximated by linear functions of $\vec{x}$ (which makes F quadratic) of the form:

$$\vec{\phi} \simeq J^T \vec{x} + \vec{c} \tag{2}$$

where J and $\vec{c}$ are a constant matrix and vector respectively. However the technique, once derived, will be applied to more general cases where $\vec{\phi}$ are highly nonlinear functions of $\vec{x}$. The constraints are approximated by a general quadratic of the form:

$$g_i(\vec{x}) \simeq \frac{1}{2} \vec{x}^T A_i \vec{x} + \vec{b}_i^T \vec{x} - d_i \leq 0 \quad i=1,\ldots,k \tag{3}$$

The gradient of the objective function (1) is given by:

$$\nabla F(\vec{x}) = 2J\vec{\phi} \tag{4}$$

which is exact whether $\vec{\phi}$ is linear or not, as long as J is the matrix of first partial derivatives of $\vec{\phi}$. The matrix of second partial derivatives of the objective function is:

$$G = 2JJ^T \tag{5}$$

which is exact only when $\vec{\phi}$ is linear. At any given iteration we assume there are ℓ active constraints (ordered such that $j = 1,2,\ldots,\ell$) where $\ell \leq k$. Thus, the Kuhn-Tucker conditions are:

$$\nabla F(\vec{x}) + (A_1\vec{x} + \vec{b}_1)\lambda_1 + \ldots + (A_\ell\vec{x} + \vec{b}_\ell)\lambda_\ell = 0 \tag{6}$$

$$g_j(\vec{x}) = \frac{1}{2} \vec{x}^T A_j \vec{x} + \vec{b}_j^T \vec{x} - d_j = 0 \quad j=1,\ldots,\ell \tag{7}$$

$$\lambda_j \geq 0 \quad j=1,\ldots,\ell$$

Similar to the development of Paradis and Willmert [3], the new

4

method is generated such that a single iteration yields the optimal de-
sign for a quadratic objective function assuming that the constraints
active at the optimal design are also active at the starting point. If
$F(\vec{x})$ is quadratic then the following equation is valid for any two points
$\vec{x}_{\nu+1}$ and $\vec{x}_{\nu}$:

$$\nabla F(\vec{x}_{\nu+1}) - \nabla F(\vec{x}_{\nu}) = G(\vec{x}_{\nu+1} - \vec{x}_{\nu}) \qquad (9)$$

Solving equation (6) for $\nabla F(\vec{x}_{\nu+1})$, assuming $\vec{x}_{\nu+1}$ is the optimal design,
and substituting into equation (9) results in the iterative expression
(after solving for $\vec{x}_{\nu+1}$):

$$\vec{x}_{\nu+1} = (G + \sum_{j=1}^{\ell} A_j \lambda_j)^{-1} [G\vec{x}_{\nu} - \sum_{j=1}^{\ell} \vec{b}_j \lambda_j - \nabla F(\vec{x}_{\nu})] \qquad (10)$$

If the objective function has the special form of equation (1), then
the G matrix in the iterative equation would be replaced by equation (5),
i.e. $G = 2JJ^T$. Otherwise, the method could still be applied as long as
the matrix of second partial derivatives G, or an approximation to it,
were known.

In order to use the iterative equation (10) the unknown vector of
Lagrange multipliers $\vec{\lambda}$ must be determined. This is accomplished by sub-
stituting the expression for $\vec{x}_{\nu+1}$, equation (10), into each of the active
constraints of equation (7) resulting in a system of ℓ nonlinear equa-
tions in ℓ unknowns $\vec{\lambda}$ of the form:

$$g_i(\vec{\lambda}) = \frac{1}{2} \left\{ (G + \sum_{j=1}^{\ell} A_j \lambda_j)^{-1} [G\vec{x}_\nu - \sum_{j=1}^{\ell} \vec{b}_j \lambda_j - \nabla F(\vec{x}_\nu)] \right\} A_i$$

$$\left\{ (G + \sum_{j=1}^{\ell} A_j \lambda_j)^{-1} [G\vec{x}_\nu - \sum_{j=1}^{\ell} \vec{b}_j \lambda_j - \nabla F(\vec{x}_\nu)] \right\}$$

$$+ \vec{b}_i^T (G + \sum_{j=1}^{\ell} A_j \lambda_j)^{-1} [G\vec{x}_\nu - \sum_{j=1}^{\ell} \vec{b}_j \lambda_j - \nabla F(\vec{x}_\nu)]$$

$$- d_i = 0 \qquad\qquad i=1,\ldots,\ell \qquad\qquad (11)$$

This system of equations in $\dot{\vec{\lambda}}$ could be solved using several dif-
ferent methods. The approach used in this research was as follows. At
each iteration initially the Newton-Raphson technique was applied. If
the method did not converge, which may be caused by the fact that the
equations had no solution or that the method simply was not able to
locate one, then another approach was used. In this case, an objective
function H was formed which was the sum of the squares of the
active constraints g_i. This unconstrained function was minimized with
respect to $\vec{\lambda}$. In this work, Powell's method was used, but any available
technique could be applied. The optimal values of $\vec{\lambda}$ (whether H is zero
or not for these values of $\vec{\lambda}$) were then used in the iterative equation
(10).

As in the original Gauss Constrained Technique (as well as the gra-
dient projection method) the criterion for dropping a constraint from the
set of active constraints is the sign of λ_i. At any iteration the con-
straint corresponding to the most negative λ is dropped from the set of
active constraints and a new vector of Lagrange Multipliers is deter-
mined. This procedure is repeated until all $\lambda_i \geq 0$. If this results in
no active constraints, then the optimization technique continues by set-

ting all $\lambda_i = 0$ in equation (10). In this case, the iterative expression,
can be shown to reduce to Gauss' method for unconstrained optimization:

$$\vec{x}_{\nu+1} = \vec{x}_\nu - (JJ^T)^{-1}J\vec{\phi} \tag{12}$$

At each iteration a decision must be made as to whether or not a new
constraint should be added to the set of active constraints. If the
direction of minimization $\vec{s}_{\nu+1}$ is defined as the direction from $\vec{x}_\nu$ to
$\vec{x}_{\nu+1}$, then a constraint is added only if a step in the $\vec{s}_{\nu+1}$ direction
will not satisfy the constraint.

Two different methods were used to handle violated constraints.
The first approach was to do nothing special if a constraint became
violated as a result of an iteration based on equation (10). Thus
whether a constraint is only active, i.e. $g_i = 0$, or if it is violated,
i.e. $g_i > 0$, it is treated the same in the optimization technique. The
basis behind this approach was the assumption that eventually the method
will satisfy all constraints, since these are equations (11) which the
method attempts to satisfy at each iteration. This approach allows the
optimization to start at any design whether it satisfies the constraints
or not.

The other method of handling violated constraints was to start at
a point which satisfied all constraints. Then if a step is taken using
equation (10) such that $g_r(\vec{x}_{\nu+1}) > 0$, a new design $\vec{x}'_{\nu+1}$ was found along
the line connecting $\vec{x}_\nu$ and $\vec{x}_{\nu+1}$ such that $g_r(\vec{x}'_{\nu+1}) \simeq 0$. This was
accomplished by stepping back from a violated constraint using the
approximate equation:

$$\vec{x}'_{\nu+1} = \vec{x}_{\nu} - \frac{(\vec{x}_{\nu+1} - \vec{x}_{\nu})g_r(\vec{x}_{\nu})}{g_r(\vec{x}_{\nu+1}) - g_r(\vec{x}_{\nu})} \qquad (13)$$

The design $x'_{\nu+1}$ was then used in the next iteration.

Although the technique was developed assuming linear functions $\vec{\phi}(\vec{x})$, i.e. $F(\vec{x})$ quadratic, the method is applicable to problems where the ϕs are general functions of $\vec{x}$. An especially important characteristic for mechanism design is that the technique requires a total of only one more objective function evaluation than iterations to obtain an optimal design, unlike the GRG Technique of Lasdon et.al [2], where a step length determination is required at each iteration.

Example Problems

Several examples were considered in this work, two of which are presented here.

The first problem, which is a modified Rosen-Suzuki test problem, consists of a quadratic objective function in eight variables with seven quadratic inequality constraints as follows:

Minimize

$$F(\vec{x}) = x_1^2 + \frac{3}{2}x_2^2 + \frac{1}{2}x_3^2 + 3x_4^2 + 2x_5^2 + \frac{5}{2}x_6^2 + x_7^2 + \frac{3}{2}x_8^2 + 2x_1$$

$$- 3x_2 + 5x_4 + x_5 + 7x_6 - 2x_7 - x_8$$

subject to:

$$g_1(\vec{x}) = \frac{1}{2}x_1^2 + \frac{3}{2}x_3^2 + 2x_4^2 - \frac{1}{2}x_7^2 + x_8^2 - 2x_3 - 4x_6 + 5x_7$$

$$- 10 \leq 0$$

$$g_2(\vec{x}) = x_1^2 + x_2^2 + x_3^2 + x_4^2 + x_5^2 + x_6^2 + x_7^2 + x_8^2 + x_1$$

$$- x_2 + x_3 - x_4 + x_5 - x_6 + x_7 - x_8 - 6 \leq 0$$

$$g_3(\vec{x}) = x_1^2 + 2x_2^2 + x_3^2 + 2x_4^2 + x_5^2 + 2x_6^2 + x_7^2 + 2x_8^2$$

$$- x_1 - x_4 - x_5 - x_8 - 13 \leq 0$$

$$g_4(\vec{x}) = x_1^2 + 2x_2^2 + 3x_3^2 + 4x_5^2 + 5x_6^2 + 6x_7^2 + x_1 - x_3$$

$$- x_5 - x_7 - 5 \leq 0$$

$$g_5(\vec{x}) = x_1^2 + x_8^2 - x_1 - x_8 - 11 \leq 0$$

$$g_6(\vec{x}) = 2x_1^2 - 2x_2^2 + 2x_3^2 - 2x_4^2 + 3x_5^2 - 3x_6^2 + 3x_7^2 - 3x_8^2$$

$$- 2x_1 + 2x_2 - 2x_3 - 2x_6 + 2x_7 - 2x_8 - 10 \leq 0$$

$$g_7(\vec{x}) = 4x_2^2 - 4x_4^2 + 2x_6^2 - 2x_8^2 - 5x_1 - 5x_3 + 5x_5$$

$$+ 5x_7 - 20 \leq 0$$

Tables 1 and 2 show the results of the optimization from two different starting points. Three different techniques were applied. The first two were variations of the Gauss Nonlinearly Constrained method. The first one, labeled GNLC.NS in the tables, ignored violated constraints, while the second, labeled GNLC, treated violated constraints using equation (13). Both of these methods were compared with the Generalized Reduced Gradient technique, labeled GRG.

Table 1 shows the results from a starting point where no constraints were active or violated. All three methods produced the same optimal design. The number of iterations NI, and number of function evaluations NF for the GNLC methods were considerably less than for the GRG. Table 2 shows the results from a starting point in which three constraints were violated, while one was active. For this starting point only the GNLC.NS technique was applicable. Again the number of iterations and function evaluations were less than for the GRG.

The second example consists of the design of a four-bar mechanism such that the coupler point (XX,YY) of the mechanism closely generated the curve defined by the eight points as shown in Figure 1. The objective function to be minimized is the sum of the distances (squared) between the desired curve and the actual curve generated by the mechanism:

$$F(\vec{x}) = \sum_{i=1}^{8} (XX_i - XG_i)^2 + (YY_i - YG_i)^2$$

where:

$$XX_i = x_2 \cos\gamma_i + x_5 \cos\psi_i + x_{10}$$

$$YY_i = x_2 \sin\gamma_i + x_5 \cos\psi_i + x_9$$

$$\psi_i = x_6 + x_7 + \eta_i - \varepsilon_i$$

$$\varepsilon_i = \tan^{-1}\left[\frac{x_2 \sin(\gamma_i - x_6)}{x_1 - x_2 \cos(\gamma_i - x_6)}\right]$$

$$\eta_i = \cos^{-1}\left[\frac{x_1^2 + x_2^2 + x_3^2 - x_4^2 - 2x_1 x_2 \cos(\gamma_i - x_6)}{2x_3 \left[x_1^2 + x_2^2 - 2x_1 x_2 \cos(\gamma_i - x_6)\right]^{1/2}}\right]$$

$$\gamma_i = x_8 + \Delta\gamma_i$$

and (XG,YG) are the coordinates of the desired curve.

The design variables $x_1,\ldots,x_{10}$ are link lengths, orientation of some of the links as well as the location of the crank pin. Note, the objective function is a highly nonlinear function of the design variables. This is the same problem that Paradis and Willmert [3] solved, however, two nonlinear constraints, g_{13} and g_{14}, have been introduced here to constrain the location of the crank pin to two user defined circular regions. Thus, our design problem contains ten variables, $x_1,\ldots,x_{10}$, and fourteen inequality constraints $g_i(\vec{x}) \leq 0$ $i=1,\ldots,14$. The constraints are:

$$g_1(\vec{x}) = 1 - x_2 \leq 0 \qquad\qquad g_8(\vec{x}) = x_2 + x_4 - x_1 - x_3 \leq 0$$

$$g_2(\vec{x}) = 1 - x_5 \leq 0 \qquad\qquad g_9(\vec{x}) = x_1 - 30 \leq 0$$

$$g_3(\vec{x}) = x_2 - x_1 \leq 0 \qquad\qquad g_{10}(\vec{x}) = x_3 - 30 \leq 0$$

$$g_4(\vec{x}) = x_2 - x_3 \leq 0 \qquad\qquad g_{11}(\vec{x}) = x_4 - 30 \leq 0$$

$$g_5(\vec{x}) = x_2 - x_4 \leq 0 \qquad\qquad g_{12}(\vec{x}) = x_5 - 30 \leq 0$$

$$g_6(\vec{x}) = x_1 + x_2 - x_3 - x_4 \leq 0 \qquad g_{13}(\vec{x}) = (x_{10} - CX_1)^2 + (x_9 - CY_1)^2$$
$$- R_1^2 \leq 0$$

$$g_7(\vec{x}) = x_2 + x_3 - x_1 - x_4 \leq 0$$

$$g_{14}(\vec{x}) = (x_{10} - CX_2)^2 + (x_9 - CY_2)^2$$
$$- R_2^2 \leq 0$$

where CX_1, CY_1, R_1, CX_2, CY_2, and R_2 were 4, 4, 3, 7, 7, and 3 re-
spectively.

The resulting optimal designs using the GNLC and GRG methods are shown in Table 3. The optimal mechanism is shown in Figure 2. Again the Gauss Nonlinearly Constrained method required significantly fewer objective function evaluations.

Conclusions

The Gauss Nonlinearly Constrained method is an effective technique of solving nonlinear design problems. It is particularly efficient for cases in which the evaluation of the objective function is very

time consuming. Although in some instances considerable calculations must be done per iteration, the amount required is still insignificant compared to that required to do just one analysis of a complex mechanical or structural system.

The method has been applied to a variety of problems consisting of objective functions of various complexities. In all cases it has worked well. However, it has received only limited application to problems involving constraints that are more than quadratically nonlinear. It appears that further research is required for such cases.

Acknowledgements

References

1. DeRubes, M.J. and Willmert, K.D., "Optimal Design of Flexible Link Mechanisms," to be published in ASME Journal of Mechanisms, Transmissions and Automation in Design.

2. Lasdon, L.S., Waren, A.D., and Ratner, M.W., "GRG2 User's Guide," Cleveland State University, February 1982.

3. Paradis, M.J. and Willmert, K.D., "Optimal Mechanism Design Using The Gauss Constrained Method," ASME Paper No. 82-DET-91, 1982.

4. Wilde, D.J., "Error Linearization in the Least-Squares Design of Function Generating Mechanisms," Progress in Engineering Optimization, ASME, New York, 1981, pp. 33-37.

Starting Point		TECHNIQUE		
		GNLC.NS	GNLC	GRG
S T A T U S F E A S I B L E	NI	2	3	14
	NF	3	4	144
1.0	x_1	-0.8797	-0.8797	-0.8797
1.0	x_2	0.7030	0.7030	0.7030
0.0	x_3	0.1092	0.1092	0.1092
1.0	x_4	0.8333	0.8333	0.8334
0.0	x_5	-0.2015	-0.2015	-0.2016
0.0	x_6	-0.8570	-0.8570	-0.8571
0.0	x_7	0.3993	0.3993	0.3993
0.0	x_8	0.3333	0.3333	0.3334
-0.5	F	-9.520	-9.520	-9.520
-	G_{ACT}	4	4	4

Table 1: Results of Rosen-Suzuki Test Problem

Starting Point		TECHNIQUE		
		GNLC.NS	GNLC	GRG
S I T N A F A T E U A S S I B L E (STATUS INFEASIBLE) NI	NI	3	*	24
	NF	4	*	276
-1	X_1	-0.8797	*	-0.8797
-1	X_2	0.7030	*	0.7030
-1	X_3	0.1092	*	0.1092
-1	X_4	0.8333	*	0.8333
-1	X_5	-0.2015	*	-0.2015
-1	X_6	-0.8570	*	-0.8570
-1	X_7	0.3993	*	0.3993
-1	X_8	0.3333	*	0.3333
14.0	F	-9.520	*	-9.520
(2,3,4 v),7	G_{ACT}	4	*	4

(v) - violated constraint

Table 2:   Results of Rosen-Suzuki Test Problem

Starting Point		GNLC	GRG

S F
T E
A A
T S
U I
S B
  L
  E   NI
	NI	11	56

NF	NF	12	389
15.0	X_1	30.0	30.0
5.0	X_2	8.345	8.345
15.0	X_3	25.821	25.821
5.0	X_4	12.817	12.817
15.0	X_5	16.026	16.026
-0.007	X_6*	-1.063	-1.063
0.412	X_7*	1.259	1.259
1.379	X_8*	1.118	1.118
6.0	X_9	4.0	4.0
5.0	X_{10}	7.0	7.0
220.29	F	1.78349	1.78348
-	G_{ACT}	9,13,14	9,13,14

*Angle Variables (radians)

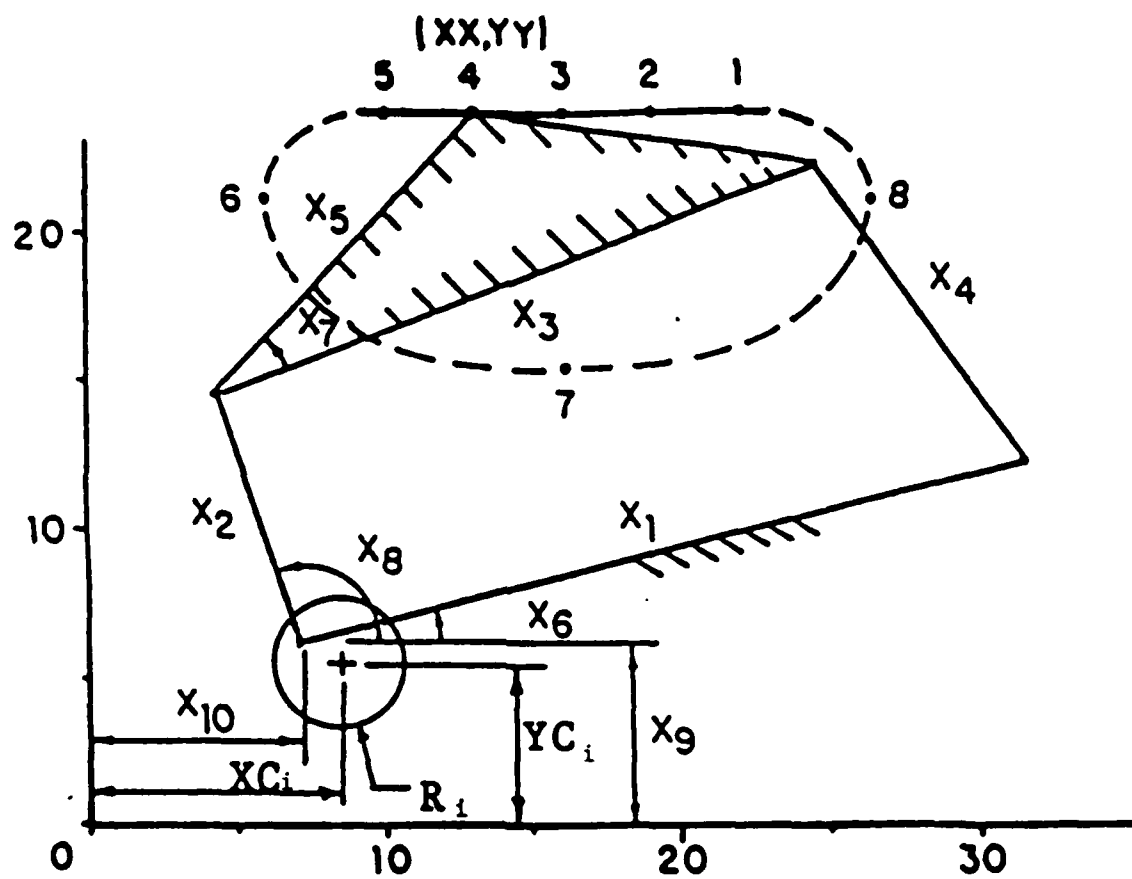Table 3: Results of Mechanism Design Problem

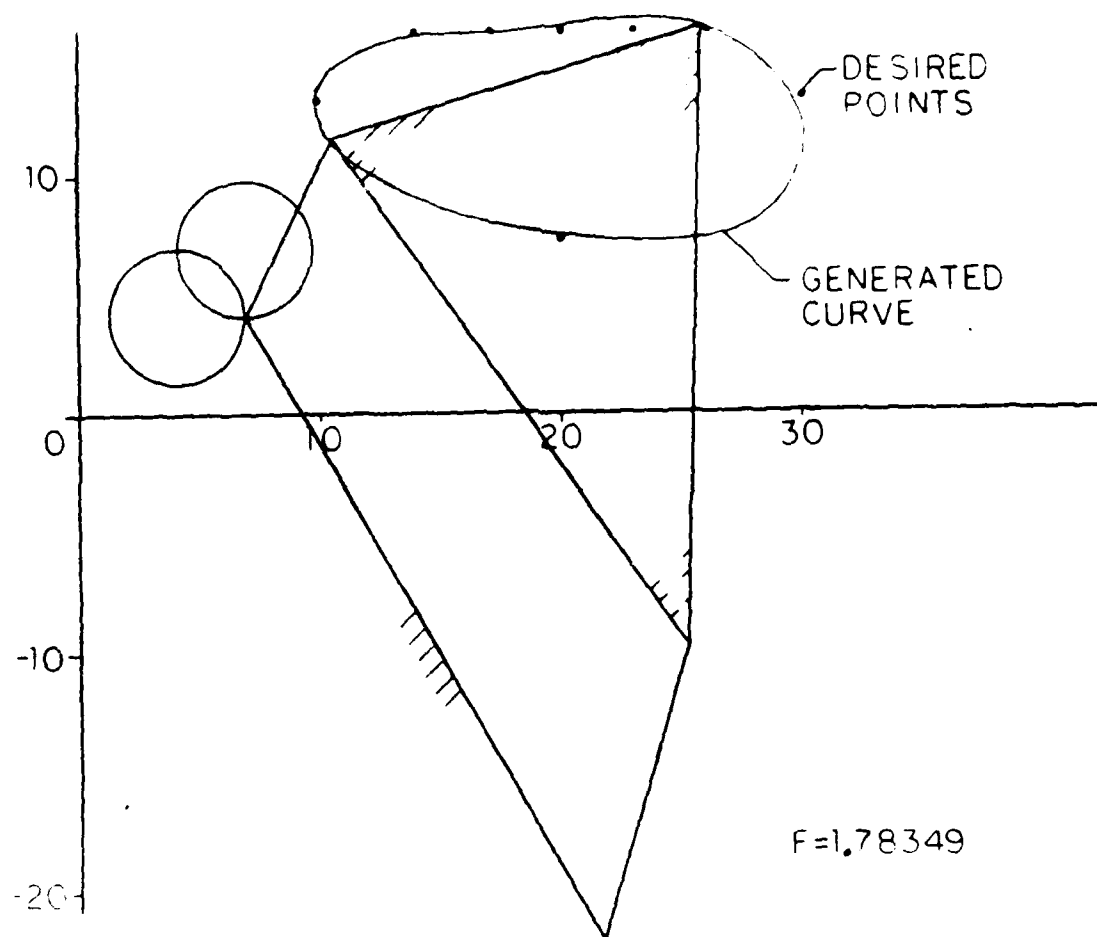Figure 1: Four-Bar Mechanism for Path Generation

Figure 2: Optimal Mechanism

FINITE ELEMENT NONLINEAR VIBRATIONAL

ANALYSIS OF PLANAR MECHANISMS

by

D. W. Tennant*
K. D. Willmert*
and
M. Sathyamoorthy*

*Department of Mechanical and Industrial Engineering
Clarkson University, Potsdam, New York, 13676

ABSTRACT

A finite element approach is presented in this paper for the nonlinear vibrational analysis of planar mechanisms. The analysis takes into account the effects of material and geometric nonlinearities on the dynamic behavior. The geometric nonlinearities included in this study are due to stretching of the neutral axis and the curvature-displacement nonlinearity, both caused by large deformations. The material nonlinearity is due to a nonlinear stress-strain relationship of the Ramberg-Osgood type. The analysis presented here makes use of hermite polynomials which ensure compatibility of curvature between elements. Using a variable correlation table, a global system of nonlinear equations are derived in terms of the global unknowns and the kinematics of the mechanism. A harmonic series technique is then used to obtain the steady state solutions to this system of nonlinear equations. Numerical results are presented for an example mechanism and the effects of the nonlinearities are discussed.

1

INTRODUCTION

The importance of flexibility of linkages on the performance of high-speed minimum-mass mechanisms is well recognized. A considerable amount of research has been done in this area in the last two decades. While it is desirable to develop analytical and numerial procedures that enable the design of rigid link mechanisms and robots to perform a given function with specified reliability, it is also important to evaluate the effects of flexibility of elastic members on their performance. It is known that a mechanism designed for operation at low speeds may not perform satisfactorily at high speeds due to the effects of large inertia forces and resulting elastic deformations. Thus it becomes necessary to include in the dynamic analysis of mechanisms, not only the effect of the rigid body motion, but also the flexibility of the linkages.

Most of the previous investigations in the area of elastic analysis of mechanisms have been carried out within the framework of the linear theory [1-16]. However, Viscomi and Ayre [17] used a Galerkin-type nonlinear analysis procedure to study the vibrations of a slider-crank mechanism. A later work by Sadler and Sandor [18] used the lumped parameter approach to a nonlinear dynamic model of an elastic linkage. The mechanism analysed in this paper was a general four-bar linkage and the analytical model inc'uded the response coupling associated with both tne transmission of forces at the pin joints and the dependence of the undeformed motion of a link on the elastic motion of other links. A finite element analysis, with the aid of

2

the piecewise linear method of Martin, was used by Sevak and McLarnan [19] to carry out the nonlinear analysis of a mechanism. Further nonlinear work dealing with the vibrations of elastic mechanisms are reported in References [20-22]. In a recent investigation, Thompson and Sung [23] used a variational formulation for the nonlinear finite element analysis of planar mechanisms considering geometric nonlinearities. Some experimental results were presented.

This paper is concerned with the nonlinear vibrational analysis of general planar mechanisms. A finite element method is used which includes the effects of both geometric and material nonlinearites. The geometric nonlinearities included in this study are due to stretching of the neutral axis with partially constrained ends and a general curvature-displacement relationship, both caused by large deformations. The material nonlinearity is of the Ramberg-Osgood type with three parameters to represent the nonlinear stress-strain relationship [24-26]. Additional effects considered are transverse shear and rotatory inertia and changes in cross-section due to realistically proportioned members. The governing nonlinear differential equations are derived for each element in terms of the axial and transverse deformations, rotations, curvatures, and shear deformation angles. These equations are then assembled with the aid of a variable correlation table and the resulting global system of equations is solved using an iterative technique based on a harmonic series solution procedure.

FINITE ELEMENT FORMULATION

A finite element method is presented below for the nonlinear analysis of a general closed looped mechanism. The mechanism can be composed of various combinations of simple four bar chains, frame elements, sliders moving on fixed references, or sliders moving on rotating links. Each link is divided into one or more elements with each element having the local coordinate system as shown in Figure 1. If a slider is present, the masses M_1 and M_2 are located at ends 1 and 2, as shown. The length of the element Δ is constant except for links with sliders moving along them.

The displacement vector of any point (a) on the element's neutral axis is given by:

$$S = (X_1 \cos\gamma + Y_1 \sin\gamma + x + u)i + (Y_1 \cos\gamma - X_1 \sin\gamma + w)j \qquad (1)$$

where X_1 and Y_1 are the coordinates of end 1 of the element given by the rigid body motion. The coordinate x is measured along the element's neutral axis from 1 to 2 and γ is the angle between the rigid body position and the X-axis. The axial and transverse displacements of point (a) from the rigid body position are given by u and w, respectively. This equation takes into account both the rigid body motion and the elastic displacements and defines the position of any point along the neutral axis.

Differentiating Equation 1 with respect to time yields the velocity of any point (a). The unit vectors i and j move with the coordinate system and

4

vary with time. The angular velocity of any differential line segment on
the neutral axis of the element is given by:

$$\gamma,_t + w,_{xt} \tag{2}$$

where $\gamma,_t$ is the derivative of γ with respect to time and $w,_{xt}$ is the de-
rivative of the transverse displacement with respect to the local coordinate
x and time t.

The kinetic energy due to rotation of the element is given by:

$$K.E._R = \frac{1}{2} \int_{-\frac{h}{2}}^{\frac{h}{2}} \int_o^\Delta \left[\rho A_x |S,_t|^2 + \rho I_z (\gamma,_t + w,_{xt})^2\right] dx\ dy$$

$$+ \frac{1}{2} M_1 |S,_t|^2_{x=o} + \frac{1}{2} M_2 |S,_t|^2_{x=\Delta} \tag{3}$$

where ρ is the mass density and A_x and I_z are the cross sectional area and
moment of inertia of the element respectively. The term $\rho I_z (\gamma,_t + w,_{xt})^2/2$
represents the effect of rotatory inertia. The kinetic energy due to beam
bending associated with transverse shear is [27].

$$K.E._B = \frac{1}{2} \int_{-\frac{h}{2}}^{\frac{h}{2}} \int_o^\Delta \{\alpha,_t^2 I_z\} dx\ dy \tag{4}$$

where α is a measure of the transverse shear angle.

5

$$U = \int_{vol} \int_o^\varepsilon \sigma \, d\varepsilon \, dvol + \int_{vol} \frac{1}{2} \tau_{xy} \gamma_{xy} \, dvol \qquad (5)$$

where σ, ε, τ_{xy}, and γ_{xy} are the normal stress, normal strain, shear stress and shear strain, respectively. For a nonlinear material of the Ramberg-Osgood type [24-26], the relationship between stress and strain is:

$$\sigma = A \varepsilon - B \varepsilon^m \qquad (6)$$

where A corresponds to Young's modulus E, and $B\varepsilon^m$ represents the nonlinear term. A, B and m are constants for the particular material being considered. The above relationship, Equation 6, is valid only for positive strains. If the strain is negative, the following expression is used:

$$\sigma = A \varepsilon + B (-\varepsilon)^m \qquad \text{if } \varepsilon < 0 \qquad (7)$$

The change in sign of the nonlinear term results in the same overall effect on the stress-strain relationship as for positive strain, i.e. either hardening or softening depending on the values of B and m.

Using the Ramberg-Osgood relationship, the following expression for the strain energy is obtained for positive strain $\varepsilon \geq 0$:

$$U = \int_{-\frac{h}{2}}^{\frac{h}{2}} \int_o^\Delta \{\frac{1}{2} A \varepsilon^2 - \frac{1}{m+1} B \varepsilon^{m+1} \, dx \, dy + \int_{-\frac{h}{2}}^{\frac{h}{2}} \int_o^\Delta \frac{1}{2} G_{xy} \gamma_{xy}^2 \, dx \, dy \qquad (8)$$

6

where x is the axial coordinate, y is the transverse coordinate, and G_{xy} is the shear modulus. When $\varepsilon < 0$ the equation is:

$$U = \int_{-\frac{h}{2}}^{\frac{h}{2}} \int_{0}^{\Delta} \{\frac{1}{2} A \varepsilon^2 - \frac{1}{m+1} B (-\varepsilon)^{m+1}\} dx\, dy$$

$$+ \int_{-\frac{h}{2}}^{\frac{h}{2}} \int_{0}^{\Delta} \frac{1}{2} G_{xy} \gamma_{xy}^2 \, dx\, dy \qquad (9)$$

The nonlinear expression for the curvature R of a planar static beam undergoing large deformations is:

$$\frac{1}{R} = \frac{w,_{xx}}{(1 + w,_x^2)^{3/2}} \qquad (10)$$

Thus the strain is:

$$\varepsilon = -\frac{y}{R} = -\frac{y\, w,_{xx}}{(1 + w,_x^2)^{3/2}} \qquad (11)$$

Combining the geometric nonlinearities due to stretching of the neutral axis and the curvature-dispalcement nonlinearity, results in the expressions for normal and shear strain:

$$\varepsilon = u,_x + \frac{1}{2} D_s w,_x^2 - \frac{y\, \alpha,_x}{(1 + D_b w,_x^2)^{3/2}} \qquad (12)$$

$$\gamma_{xy} = w,_x + \alpha \tag{13}$$

Substituting these expressions for strain into the strain energy Equations (8) and (9) produces, for $\epsilon \geq 0$

$$S.E. = \int_{-\frac{h}{2}}^{\frac{h}{2}} \int_{o}^{\Delta} b\{\frac{1}{2} A (u,_x + \frac{1}{2} D_s w,_x^2 - \frac{y \alpha,_x}{(1 + D_b w,_x^2)^{3/2}})^2$$

$$+ \frac{D_k}{m+1} B (u,_x + \frac{1}{2} D_s w,_x^2 - \frac{y \alpha,_x}{(1 + D_b w,_x^2)^{3/2}})^{m+1}$$

$$+ \frac{1}{2} G_{xy} (w,_x + \alpha)^2\}dx \, dy \tag{14}$$

and when $\epsilon < 0$

$$S.E. = \int_{-\frac{h}{2}}^{\frac{h}{2}} \int_{o}^{\Delta} b \{\frac{1}{2} A (u,_x + \frac{1}{2} D_s w,_x^2 - \frac{y w,_{xx}}{(1 + D_s w,_x^2)^{3/2}})^2$$

$$- \frac{D_k}{m+1} B (-u,_x - \frac{1}{2} D_s w,_x^2 + \frac{y w,_{xx}}{(1 + D_b w,_x^2)^{3/2}})^{m+1}$$

$$+ \frac{1}{2} G_{xy} (w,_x + \alpha)^2\}dx \, dy \tag{15}$$

In Equations (12), (14) and (15), D_k, D_b and D_s are tracing constants

8

representing the effects of material nonlinearity, geometric nonlinearity due to curvature, and geometric nonlinearity due to stretching of neutral axis, respectively. Each tracing constant is equated to unity when that particular nonlinearity is being considered and is equated to zero when it is not.

In order to represent realistically proportioned members, changes in cross section are included. Each element is divided into sections of varying lengths with constant area. The intergrations involved in the element equations are carried out in a piecewise fashion with the area in each section taken as a constant. This procedure provides a reasonable approximation of variable cross sectional members without having to resort to large numbers of elements.

The Lagrange function L is defined as:

$$L = \sum_{k=1}^{S} \sum_{i=1}^{N_k} (K.E._R + K.E._B - S.E.)_{ik} \qquad (16)$$

where N_k is the total number of elements in the kth link and S is the number of links in the mechanism. Substituting Equations (3), (4) and (14) into Equation (16), the Lagrangian L can be expressed in terms of the displacements u, w, the shear angle α, and the rigid body motion.

Hermite polynomials are used to approximate u, w, and α in order to satisfy the boundary conditions of various types of mechanisms easily and to ensure interelement compatibility. The axial deformation u is approximated by a linear shape function given by

$$u = U_1(t) N_1(x) + U_2(t) N_2(x) \qquad (17)$$

9

Similarly, fifth degree polynomial shape functions are used to approximate
the transverse deformation w:

$$w = W_1(t) \ H_{11}(x) + \bar{\theta}_1(t) \ H_{21}(x) + \bar{m}_1(t) \ H_{31}(x)$$

$$+ \ W_2(t) \ H_{12}(x) + \bar{\theta}_2(t) \ H_{22}(x) + \bar{m}_2(t) \ H_{32}(x) \tag{18}$$

where θ and m are continuous between elements. The shear angle α is also
approximated by a fifth degree polynomial in order to make it compatible
with the transverse displacement w. Therefore α is assumed to be:

$$\alpha = \bar{\alpha}_1(t) \ H_{11}(x) + \bar{\psi}_1(t) \ H_{21}(x) + \bar{\lambda}_1(t) \ H_{31}(x)$$

$$+ \ \bar{\alpha}_2(t) \ H_{12}(x) + \bar{\psi}_2(t) \ H_{22}(x) + \bar{\lambda}_2(t) \ H_{32}(x) \tag{19}$$

where ψ and λ are the first and second derivatives of α, respectively.

The Hermite polynomials are given by:

$$N_1(x) = 1 - e$$
$$N_2(x) = e \tag{20}$$

$$H_{11}(x) = 1 - 10e^3 + 15e^4 - 6e^5$$

$$H_{21}(x) = \Delta(e - 6e^3 + 8e^4 - 3e^5)$$

$$H_{31}(x) = \Delta^2(e^2 - 3e^3 + 3e^4 - e^5)/2$$

$$H_{12}(x) = 10e^3 - 15e^4 + 6e^5$$

$$H_{22}(x) = \Delta(-4e^3 + 7e^4 - 3e^5)$$

$$H_{32}(x) = \Delta^2(e^3 - 2e^4 + e^5)/2 \tag{21}$$

10

where, $e = x/\Delta$.

A transformation of coordinates is now introduced to change from the moving coordinate system associated with the elements to global coordinates. Only U_1, W_1, U_2 and W_2 need to be transformed. The other coordinates are angles or derivatives of angles which are not directional on the X, Y coordinate system used. The transformations are:

$$U_1 = \bar{U}_1 \cos\phi_1 - \bar{W}_1 \sin\phi_1$$

$$W_1 = \bar{U}_1 \sin\phi_1 + \bar{W}_1 \cos\phi_1$$

$$U_2 = \bar{U}_2 \cos\phi_2 - \bar{W}_2 \sin\phi_2$$

$$W_2 = \bar{U}_2 \sin\phi_2 + \bar{W}_2 \cos\phi_2 \tag{22}$$

For pin connections the transformation angles ϕ_1 and ϕ_2 are set equal to $-\gamma$ (the rigid body angle) which transforms the coordinates back to the global coordinates. For sliders moving on rotating links the transformation becomes more involved. In this case the deformation of the driver link must be transformed to correspond to the axial and transverse deformation of the rotating link [14].

Substituting the expressions form Equation (22) into Equations (17) and (18), the global coordinates for the system are then:

$$\bar{q} = [\bar{U}_1 \; \bar{W}_1 \; \bar{\theta}_1 \; \bar{m}_1 \; \bar{\alpha}_1 \; \bar{\psi}_1 \; \bar{\lambda}_1 \; \bar{U}_2 \; \bar{W}_2 \; \bar{\theta}_2 \; \bar{m}_2 \; \bar{\alpha}_2 \; \bar{\psi}_2 \; \bar{\lambda}_2]^T \tag{23}$$

The Lagrangian function is then written in terms of the transformed element coordinates. Differentiating the Lagrangian with respect to the element coordinates, the following element equations are obtained:

11

$$\frac{d}{dt}\left(\frac{\partial L}{\partial \bar{q}_{,t}}\right) - \frac{\partial L}{\partial \bar{q}} = 0 \qquad (24)$$

In differentiating the expressions for the kinetic and strain energies in Equations (3), (4) and (14) it must be kept in mind that Δ which is the upper limit of integration is a function of time. The operations carried out in Equation (24) results in a system of nonlinear element differential equations. Assembling the element matrices for the particular mechanism being solved results in the global system of equations:

$$M\,\bar{Q}_{,tt} + C\,\bar{Q}_{,t} + (K_e + K_n)\,\bar{Q} = \bar{F}(t) \qquad (25)$$

The M, C, K_e and K_n matrices are all functions of time. The C matrix results from the kinetic energy of the system. No damping was included in the formulation of the problem. The $C\,\bar{Q}_{,t}$ term was found to be small and thus was ignored in the analysis. The matrix K_e is the linear portion of the total stiffness matrix. It is a function of rigid body motion but not a function of the deformations $\bar{Q}$. The matrix K_n, however, is the nonlinear portion of the stiffness matrix. It is a function of the deformations. Equation (25) is thus a nonlinear system of equations.

The derivation of the finite element Equation (25) is based on the assumption of positive strains ϵ. If the strain is negative a similar derivation is possible, based on Equation (15) for the strain energy rather than Equation (14). The only difference in the resulting Equation (25) is in the stiffness matrix. Wherever an ϵ^{m-1} occurs in the original formulation, it becomes $(-\epsilon)^{m-1}$ for negative strains. All other negative signs

12

resulting from the introduction of $-\epsilon$ cancelled out in the differentiations required. Thus in order to handle both positive and negative strains the terms involving ϵ^{m-1} in the stiffness matrix were replaced by $|\epsilon|^{m-1}$.

In order to solve the nonlinear system of Equation (25) an iterative approach was used. First the equations were solved using the linear terms only, i.e. the K_n matrix was ignored. This was accomplished by setting all of the tracing constants D_b, D_s and D_k equal to zero. The solution $\bar{Q}$ for the linear equations was then used to determine values for the nonlinear stiffness matrix K_n. Equation (25) was then solved again for new values for $\bar{Q}$, and the process repeated. Experience showed that this procedure converged in from 3 to 5 iterations. To solve Equation (25) for $\bar{Q}(t)$, for particular K_n, a harmonic series solution method was used similar to that of Bahgat and Willmert [14]. This approach overcomes problems with stability, due to the time varying nature of the matrices, that sometimes result from an eigenvalue technique. The steady state solution is obtained without adding artificial damping. The solution, without the $C\ \bar{Q}_{,t}$ term, is given by:

$$\bar{Q}(t) = \sum_{n=0}^{N} (K - n^2 \omega^2 M)^{-1} (\bar{A}_n \cos n\omega t + \bar{B}_n \sin n\omega t) \tag{26}$$

where ω is the input crank speed, and $\bar{A}_n$ and $\bar{B}_n$ are solutions to the linear equations:

$$\bar{F}(t_k) = \sum_{n=0}^{N} \bar{A}_n \cos n\omega t_k + \sum_{n=0}^{N-1} \bar{B}_n \sin n\omega t_k$$

$$\text{for } k = 0,1,\ldots,2N-1 \tag{27}$$

where $\bar{A}_o$ is set equal to zero. The values of t_k are the times at 2N equal time increments per revolution of the input crank given by

$$t_k = \frac{\pi k}{N\omega} \qquad \text{for } k = 0,1,\ldots,2N-1 \qquad (28)$$

Computational experience indicates that a fairly accurate solution is obtained using only a few terms in Equation (26). As the number of terms increases the components of the matrix $(K - n^2 \omega^2 M)$ grow and thus the inverse $(K - n^2 \omega^2 M)^{-1}$ becomes small. The summation can therefore be truncated to reduce computational time.

The stress in the links is calculated by evaluating the strains from Equation (12). The stress can then be determined at any point in an element using Equations (6) or (7). To find the maximum stress in an element the maximum strain must be found. Setting the first derivative of Equation (12) to zero and solving the resulting expression, the position of the maximum strain is determined. Once the location is known, the maximum strain and stress can be evaluated.

The above formulation is based on the use of the shear angle α, which is appropriate particularly for short members. For long slender links this quantity is not required. The elimination of α reduces the size of the problem considerably since the nodal deformations α_1, ψ_1, λ_1, α_2, ψ_2 and λ_2 would no longer be present. For long slender members:

$$\alpha \simeq - w,_x \qquad (29)$$

Using this expression, the equation for strain energy (14) for positive

shear ϵ reduces to:

$$S.E. = \int_{-\frac{h}{2}}^{\frac{h}{2}} \int_{o}^{\Delta} b \left\{ \frac{1}{2} A \left(u,_x + \frac{1}{2} D_s w,_x^2 + \frac{y \, w,_x}{(1 + D_b w,_x^2)^{3/2}} \right)^2 \right.$$

$$\left. - \frac{D_k}{m+1} B \left(u,_x + \frac{1}{2} D_s w,_x^2 + \frac{y \, w,_x}{(1 + D_b w,_x^2)^{3/2}} \right)^{m+1} \right\} dx \, dy \qquad (30)$$

A similar expression exists for negative strain. The kinetic energy also

changes if α is not present. The energy associated with transverse shear,

Equation (4), is eliminated and thus Equation (3) represents the total

kinetic energy of the element. Using a procedure similar to the method

outlined above, vibrational equations of the same form as Equation (25) can

be obtained, but they will be smaller in size. However, nonlinear terms

still exist in the stiffness matrix due to the material and geometric non-

linearities. The method of solution is thus identical to that outlined

earlier.

EXAMPLE PROBLEM

The following example is presented to illustrate the method of solution. The nonlinearities due to neutral axis stretching, curvature-displacement and stress-strain relationship are all considered. A four-bar linkage, as shown in Figure 2, is used as the example with all the members flexible and made of the same material. The data for the mechanism is

Length of input crank (AB) = 5.0 in

Length of coupler (BC) = 11.0 in

Length of rocker (CD) = 10.5 in

Fixed distance (AD) = 10.0 in

Cross section of links = rectangular

Height of rectangle = 1.0 in

Width of rectangle = 0.25 in

The initial position of the input crank is zero degrees at t = 0 and the direction of rotation is counterclockwise. The mechanism is divided into three elements with each link in the mechanism taken as an element. The boundary conditions are that only moment and shear terms exist for the input crank's driven end (A). For the pin connections between links, there are deformations, rotations and shear terms, and for the rocker's fixed point there are only rotation and shear terms.

First, the deformations in the mechanism were determined with the shear

angle α present. In this case the crank link was rotated at 100 rad/sec. The material properties, approximating aluminum, were as follows:

$A = 10.87 \times 10^6$ lb/in^2

$B = 0.8387 \times 10^{11}$ lb/in^2

$m = 3.0$

Mass density = 0.0002536 lb-sec^2/in^4

Three separate procedures were used to obtain numerical results. First the problem was solved using the linear analysis method of Bahgat and Willmert [14], with $E = A$. Next the method of this paper was used with the tracing constants equal to zero. Thus a linear analysis was obtained. Finally the method was applied with all tracing constants equal to one, i.e. a full nonlinear analysis. A representative deformation $\bar{U}_1$ as a function of crank position is shown in Figure 3. This is the horizontal deformation of the free end of the crank link. As can be seen, the three curves are very similar. The effect of the shear angle α is to increase the deformation slightly. For this slow speed the linear and nonlinear analyses were almost identical.

The same problem was solved again at a higher speed of 200 rad/sec. The resulting deformation $\bar{U}_1$ is shown in Figure 4. As can be seen, high frequency oscillations started to appear, with greater separation between the three analyses. At even higher speed these oscillations became more predominant to the point of instabilities in the analysis at very high speeds.

17

The revised form of the analysis equations was considered next, i.e.
the form without the strain angle α. Here a crank speed of 150 rad/sec was
used. A comparison was made of the effects of the various nonlinearities
on the deformations and stresses as compared to the linear analysis.
Figures 5 and 6 show a comparison of the linear and nonlinear deformations
$\bar{U}_2$ (the horizontal deformation of the free end of the output link) caused
separately by geometric and material nonlinearities. Figures 7 and 8 show
the maximum stresses in the connecting link of the mechanism. As expected,
the material nonlinearity of the Ramberg-Osgood type results in deformations
which are greater in magnitude than those obtained using a linear elastic
model. The maximum stress decreased due to the presence of the term $B\varepsilon^m$
subtracted from the linear stress expression.

The geometric nonlinearities considered, namely curvature displacement
and stretching of the neutral axis, both due to large deformations produced
mixed results with deformations reduced at some points and increased at other
points. The effect of the geometric nonlinearities would be expected to
produce a stiffening of the members [27] of the mechanism and thus produce
smaller deformations. The increased deformations in this case might be due
to the fact that the deformations are in relationship to the entire mechanism
and not just to the individual beam element.

18

CONCLUSIONS

The nonlinear analysis procedure, using a finite element technique, is an effective method of calculating the steady state deformations and stresses in a mechanism. Significant differences can occur between the linear and nonlinear approaches. This was particularly true for the stresses in the example considered in this work. Research is still needed on the overall effect of the shear angle α, and a more complete picture of the nonlinear terms in the analysis would be of value. Additional nonlinear effect should also be investigated, such as separation of the translations of one link due to large deformations of the other links.

ACKNOWLEDGEMENTS

REFERENCES

[1] Jasinski, P. W., Lee, H. C. and Sandor, G. N., "Stability and Steady-State Vibrations in a High-Speed Slider-Crank Mechanism," Journal of Applied Mechanics, Trans. ASME, Vol. 37, 1970, pp. 1069-1076.

[2] Winfrey, R. C., "Elastic Link Mechanism Dynamics," Journal of Engineering for Industry, Trans. ASME, Vol. 93, 1971, pp. 268-272.

[3] Winfrey, R. C., "Dynamic Analysis of Elastic Link Mechanisms by Reduction of Coordinates," Journal of Engineering for Industry, Trans. ASME, Vol. 94, 1972, pp. 577-582.

[4] Erdman, A. G., Sandor, G. N. and Oakberg, R. G., "A General Method of Kineto-Elastodynamic Analysis and Synthesis of Mechanisms, "Journal of Engineering for Industry, Trans. ASME, Vol. 94, 1972, pp. 1193-1205.

[5] Iman, I., Sandor, G. N. and Kramer, S. N., "Deflection and Stress Analysis in High Speed Planar Mechanisms with Elastic Links," Journal of Engineering for Industry, Trans. ASME, Vol. 95, 1973, pp. 541-548.

[6] Sadler, J. P. and Sandor, G. N., "A Lumped Parameter Approach to Vibration and Stress Analysis of Elastic Linkages," Journal of Engineering for Industry, Trans. ASME, Vol. 95, 1973, pp. 549-557.

[7] Winfrey, R. C., Anderson, R. V. and Gnilka, C. W., "Analysis of Elastic Machinery with Clearances," Journal of Engineering for Industry, Trans. ASME, Vol. 95, 1973, pp. 695-703.

[8] Chu, S. C. and Pan, K. C., "Dynamic Response of a High-Speed Slider-Crank Mechanism with an Elastic Connecting Rod," Journal of Engineering for Industry, Trans. ASME, Vol. 97, 1975, pp. 542-550.

[9] Bagci, D., "Dynamic Motion Analysis of Plane Mechanisms with Coulomb and Viscous Damping Via the Joint Force Analysis," Journal of Engineering for Industry, Trans. ASME, Vol. 97, 1975, pp. 551-560.

[10] Sadler, J. P., "On the Analytical Lumped-Mass Model of an Elastic Four-Bar Mechanism," Journal of Engineering for Industry, Trans. ASME, Vol. 97, 1975, pp. 561-565.

[11] Koster, M. P., "Effect of Flexibility of Driving Shaft on the Dynamic Behavior of a Cam Mechanism," Journal of Engineering for Industry, Trans. ASME, Vol. 97, 1975, pp. 595-602.

[12]   Dubowsky, S. and Gardner, T. N., "Dynamic Interactions of Link
       Elasticity and Clearance Connections in Planar Mechanical Systems,"
       Journal of Engineering for Industry, Trans. ASME, Vol. 97, 1975,
       pp. 652-661.

[13]   Bahgat, B. M., "General Finite Element Vibrational Analysis of Planar
       Mechanisms," Ph.D. Dissertation, Clarkson College of Technology,
       Potsdam, N.Y., Nov. 1973.

[14]   Bahgat, B. M. and Willmert, K. D., "Finite Element Vibrational
       Analysis of Planar Mechanisms," Mechanism and Machine Theory, Vol. 11,
       1976, pp. 47-71.

[15]   Khan, M. R., "Vibration of Mechanisms with Sliding Pairs Using Con-
       stant Length Finite Elements," M.S. Dissertation, Clarkson College
       of Technology, Potsdam, N.Y., Feb. 1976.

[16]   Naganathan, G., "New Finite Elements for Quasi-Static Deformations and
       Stresses in Mechanisms," M.S. Dissertation, Clarkson College of
       Technology, Potsdam, N.Y., 1980.

[17]   Viscomi, B. V. and Ayre, R. S., "Nonlinear Dynamic Response of Elastic
       Slider-Crank Mechanism," Journal of Engineering for Industry, Trans.
       ASME, Vol. 93, 1971, pp. 251-262.

[18]   Sadler, J. P. and Sandor, G. N., "Nonlinear Vibration Analysis of
       Elastic Four-Bar Linkages," Journal of Engineering for Industry, Trans.
       ASME, Vol. 96, 1974, pp. 411-419.

[19]   Sevak, N. M. and McLarnan, C. W., "Optimal Synthesis of Flexible Link
       Mechanisms with Large Static Deflections, "Journal of Engineering for
       Industry, Trans. ASME, Vol. 97, 1975, pp. 520-526.

[20]   Badlani, M. and Midha, A., "Member Initial Curvature Effects on the
       Elastic Slider-Crank Mechanism Response," Journal of Mechanical Design,
       Trans. ASME, Vol. 104, 1982, pp. 159-167.

[21]   Davidson, I., "Non-linear Effects in the Support Motion of an Elastic-
       ally Mounted Slider Crank Mechanism," Journal of Sound and Vibration,
       Vol. 86, 1983, pp. 71-83.

[22]   Sivertsen, O. I. and Waloen, A. O., "Non-linear Finite Element Form-
       ulations for Dynamic Analysis of Mechanisms with Elastic Components,"
       ASME Paper No. 82-DET-102.

[23]   Thompson, B. S. and Sung, C. K., "A Variational Formulation for the
       Nonlinear Finite Element Analysis of Flexible Linkages; Theory, Imple-
       mentation and Experimental Results," ASME Paper No. 84-DET-15, 1984.

21

[24] Ramberg, W. and Osgood, W. R., "Description of Stress-Strain Curves
      by Three Parameters," National Advisory Committee for Aeronautics,
      Technical Note No. 902, 1943.

[25] Venkateswara Rao, G. and Krishna Murty, A. V., "An Alternate Form of
      the Ramberg-Osgood Formula for Matrix Displacement Analysis," Nuclear
      Engineering and Design, Vol. 17, 1971, pp. 297-308.

[26] Papirno, R., "Goodness-of-Fit of the Ramberg-Osgood Analytic Stress-
      Strain Curve to Tensile Test Data," Journal of Testing and Evaluation,
      Vol. 10, 1982, pp. 263-268.

[27] Sathyamoorthy, M., "Large Amplitude Vibrations of Moderately Thick
      Beams," Proceedings of the First International Modal Analysis Con-
      ference, Orlando, Florida, 1982, pp. 136-140.

[28] Huang, T. C., "The Effects of Rotatory Inertia and of Shear Deforma-
      tion on the Frequency and Normal Mode Equations of Uniform Beams with
      Simple End Conditions," Journal of Applied Mechanics, Trans. ASME,
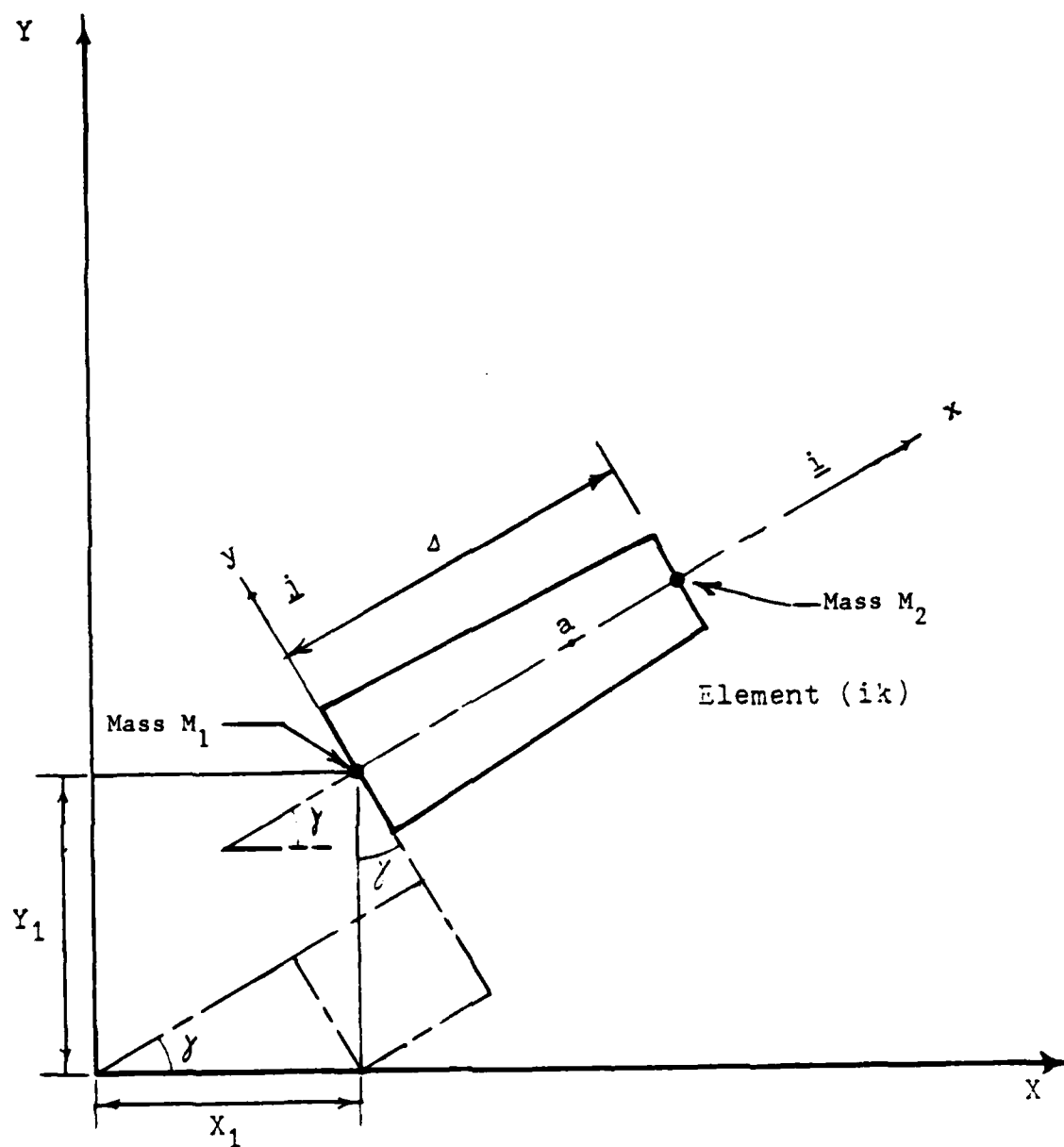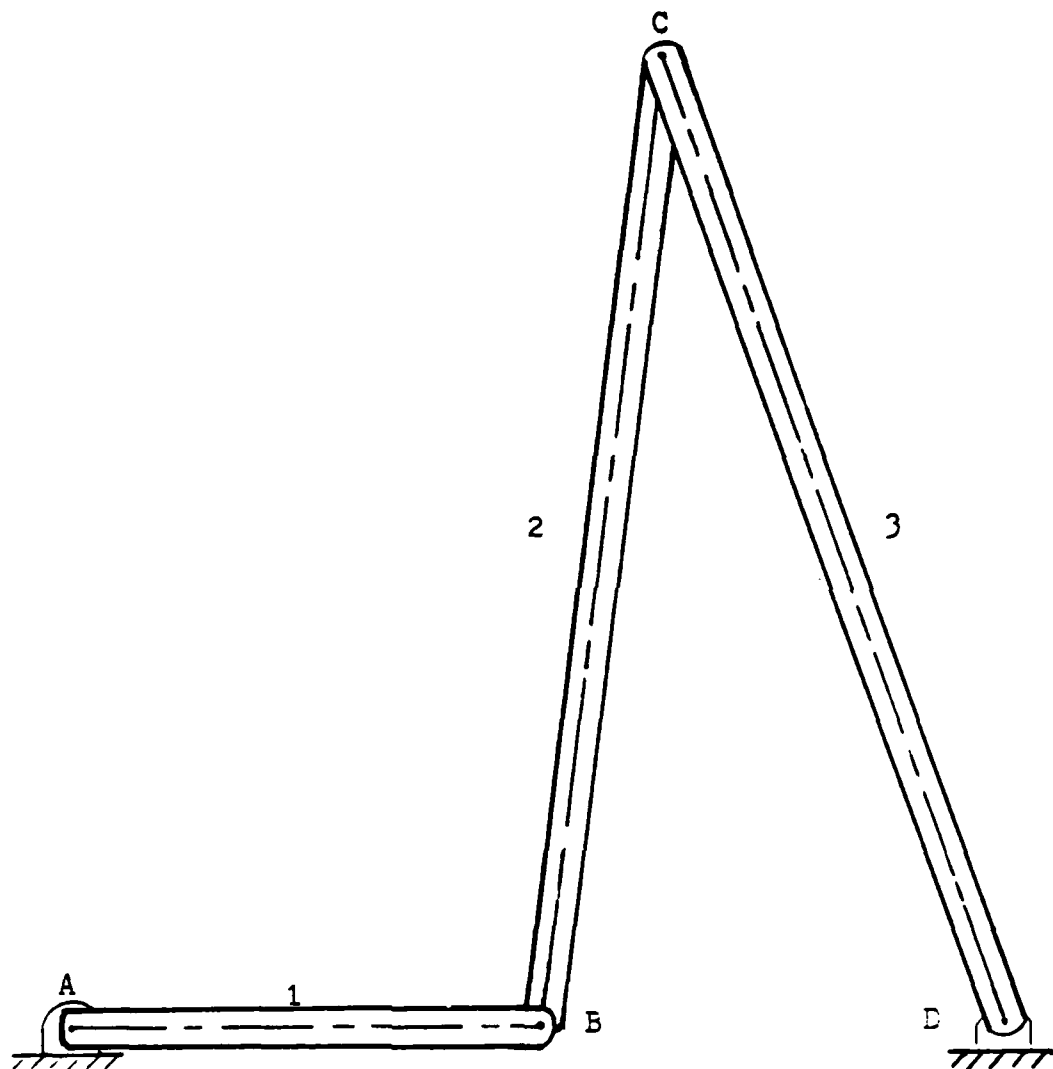   Vol. 28, 1961, pp. 579-584.

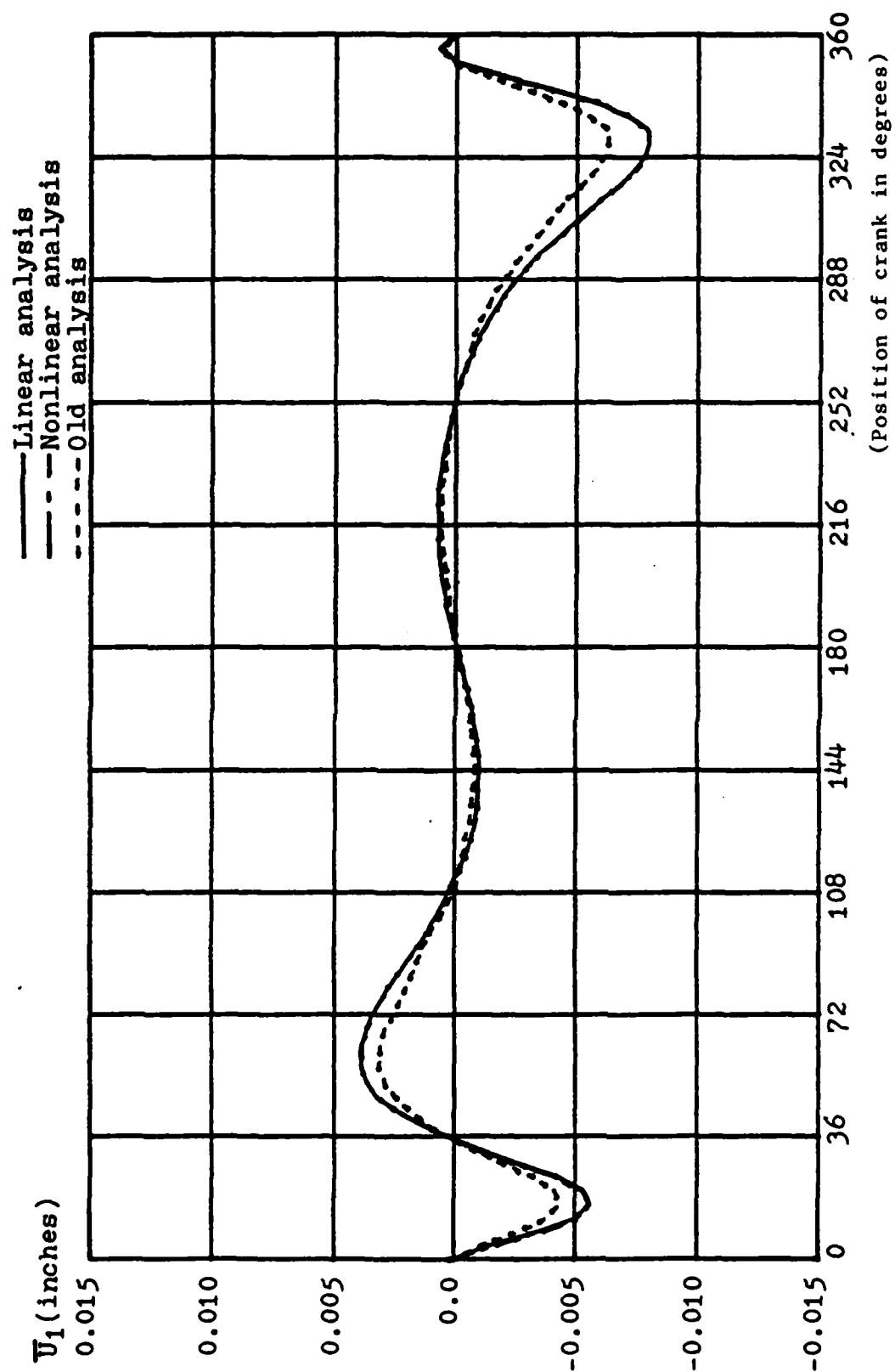Figure 1 - General Element

Figure 2 - Four Bar Mechanism

$\overline{U}_1$ (inches)

Linear analysis
Nonlinear analysis
Old analysis

0.015   0.010   0.005   0.0   -0.005   -0.010   -0.015

0   36   72   108   144   180   216   252   288   324   360

(Position of crank in degrees)

Figure 3 - Deformations $\overline{U}_1$ for Aluminum at 100 rad/sec

$\overline{U}_1$(inches)

0.030

0.0

-0.030

-0.060

-0.090

-0.120

——— Linear analysis
——— Nonlinear analysis
----- Old analysis

0   36   72   108   144   180   216   252   288   324   360

(Position of crank in degrees)
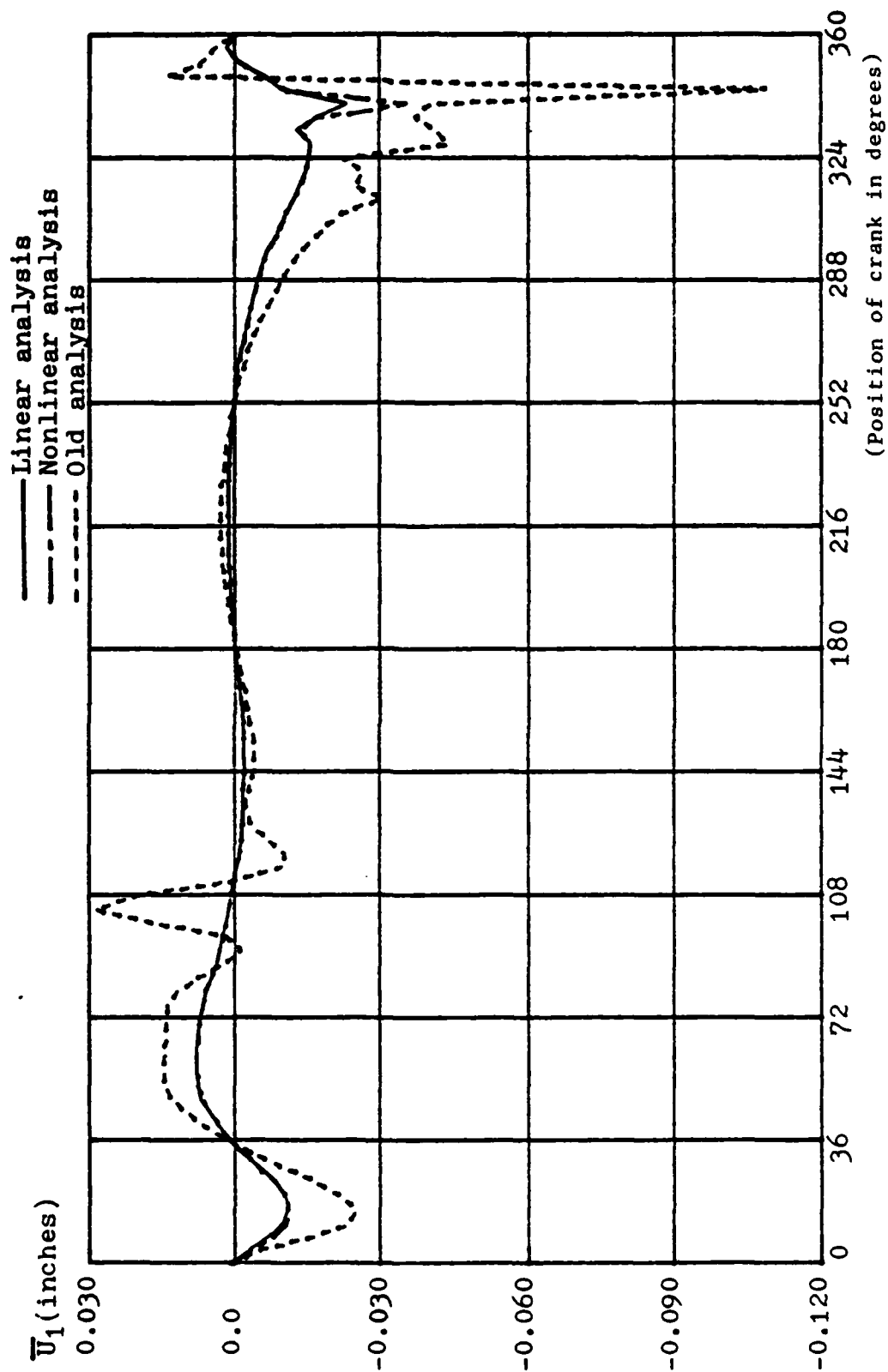
Figure 4 - Comparison of Deformations $\overline{U}_1$ at 200 rad/sec
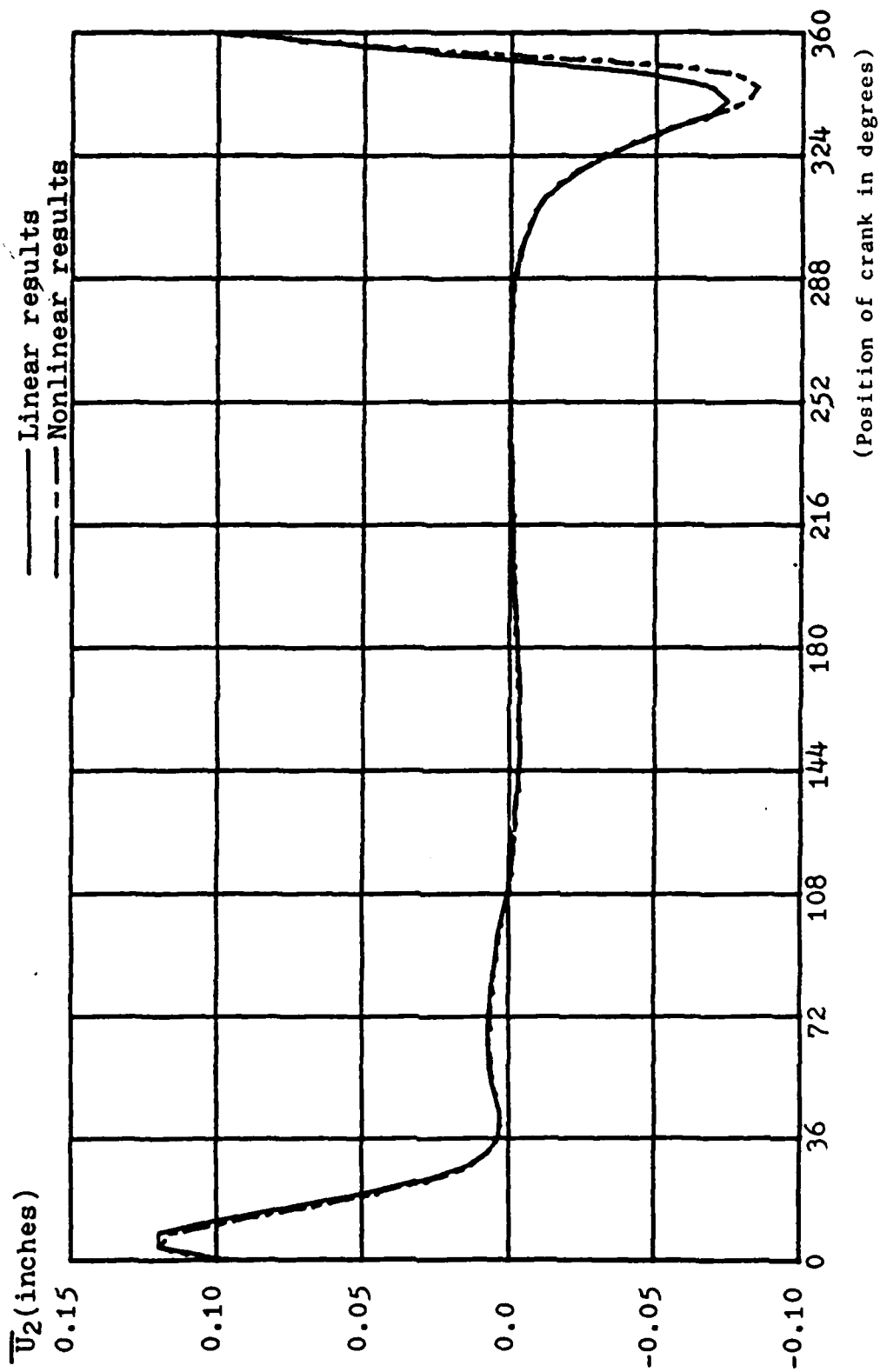
Figure 5 - Comparison of Deformations $\bar{U}_2$ at 150 rad/sec for Geometric Nonlinearities
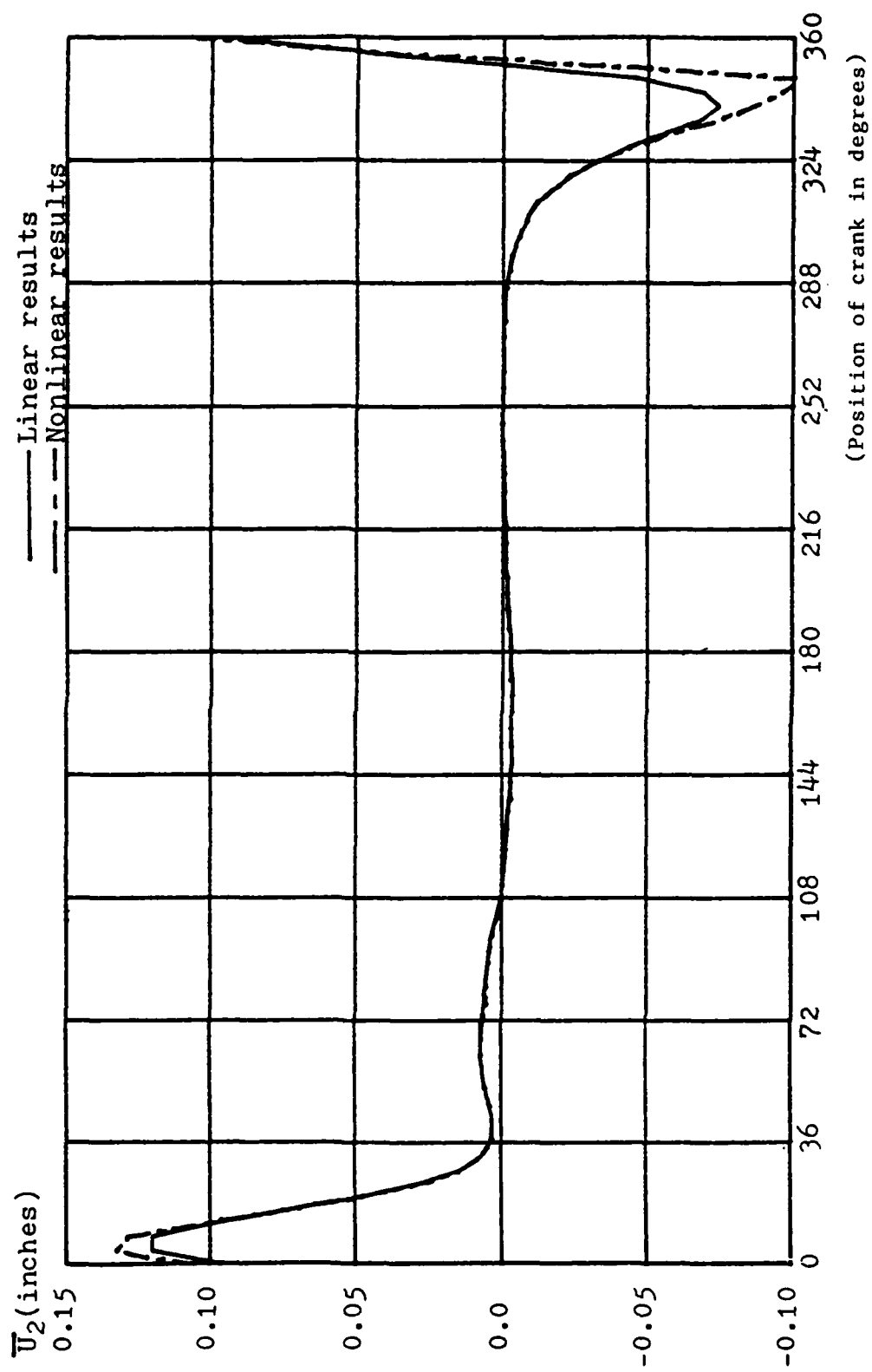
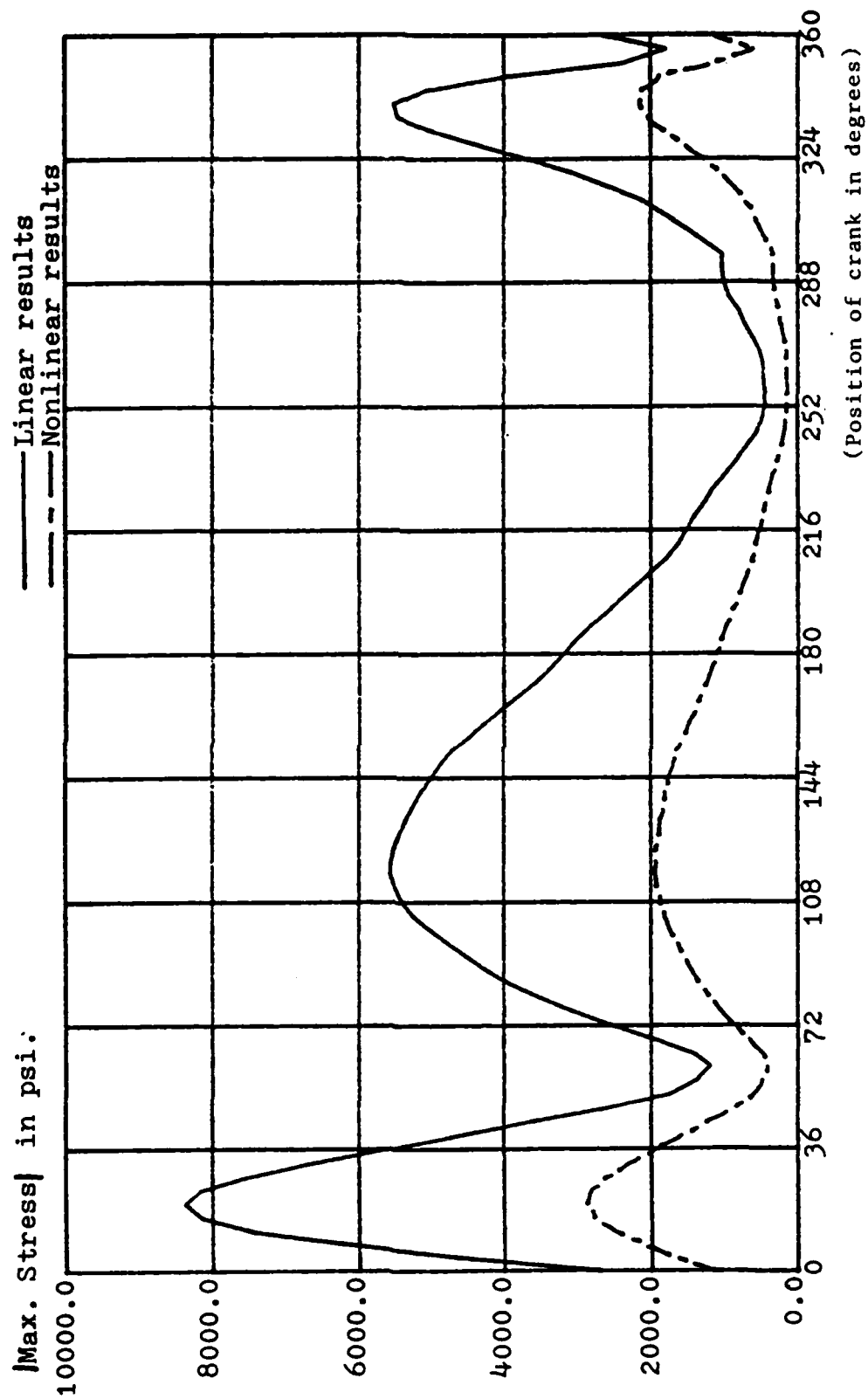Figure 6 - Comparison of Deformations $\bar{U}_2$ at 150 rad/sec for Material Nonlinearity

Figure 7 - Maximum Stresses in Element 2 at 150 rad/sec for Geometric Nonlinearities
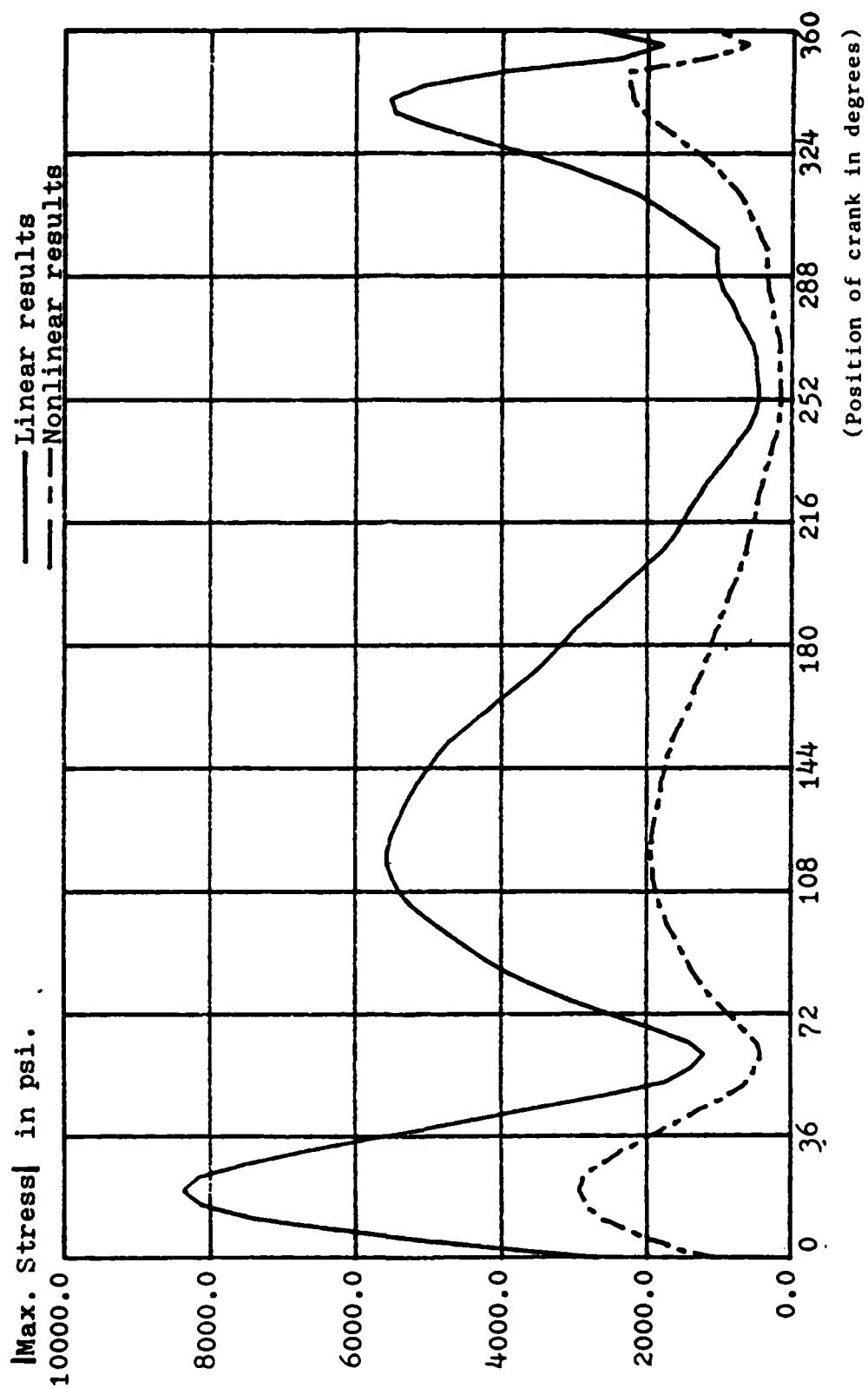
Figure 8 - Maximum Stresses in Element 2 at 150 rad/sec for Material Nonlinearity

END

FILMED

1-86

DTIC